Environmental Science and Pollution Research (2019) 26:5693–5703
https://doi.org/10.1007/s11356-018-3919-5

RESEARCH ARTICLE

Combination with catalyzed Fe(0)-carbon microelectrolysis and activated carbon adsorption for advanced reclaimed water treatment: simultaneous nitrate and biorefractory organics removal

Zhifeng Hu[1] · Desheng Li[1,2] · Shihai Deng[1,2] · Yuanhui Liu[1] · Changyue Ma[1] · Chao Zhang[1]

Received: 3 September 2018 / Accepted: 4 December 2018 / Published online: 5 January 2019

Abstract

A process combining catalyzed Fe(0)-carbon microelectrolysis (IC-ME) with activated carbon (AC) adsorption was developed for advanced reclaimed water treatment. Simultaneous nitrate reduction and chemical oxygen demand (COD) removal were achieved, and the effects of composite catalyst (CC) addition, AC addition, and initial pH were investigated. The reaction kinetics and reaction mechanisms were calculated and analyzed. The results showed that CC addition could enhance the reduction rate of nitrate and effectively inhibit the production of ammonia. Moreover, AC addition increased the adsorption capacity of biorefractory organic compounds (BROs) and enhanced the degradation of BRO. The reduction of NO_3^-–N at different pH values was consistently greater than 96.9%, and NH_4^+–N was suppressed by high pH. The presence of CC ensured the reaction rate of IC-ME at high pH. The reaction kinetics orders and constants were calculated. Catalyzed iron scrap (IS)-AC showed much better nitrate reduction and BRO degradation performances than IS-AC and AC. The IC-ME showed great potential for application to nitrate and BRO reduction in reclaimed water.

Keywords Fe(0)-carbon microelectrolysis · Composite catalyst · Activated carbon · Reclaimed water · Nitrate · Biorefractory organic compounds

Introduction

The effluent from secondary biotreatment processes in wastewater treatment plants (WWTPs) is routinely reused as reclaimed water (Chen et al. 2017; Deng et al. 2016a). Reuse of the reclaimed water for industrialization and domestic urban use is a necessary trend because of the increasing shortage of freshwater (Chen et al. 2017; Le-Minh et al. 2010). Nevertheless, the relatively high levels of residual nitrate (NO_3^-–N) and biorefractory organic compounds (BROs) are becoming a major bottleneck for reclaimed water reuse (Desheng et al. 2013; Ozgun et al. 2013). Furthermore, the direct discharge of reclaimed water into natural waters without advanced treatment is exacerbating water pollution and threatening the safety of drinking water (Cho et al. 2010; Le-Minh et al. 2010). Thus, improvement of reclaimed water quality, especially advanced removal of NO_3^-–N and degradation of BRO, is imperative.

When the readily available biochemical oxygen demand (BOD) is limited in reclaimed water in secondary biotreatment, uncommon electron donors can be utilized for biological denitrification (Deng et al. 2016a; Gao et al. 2017; He et al. 2018; Lee et al. 2011). In reclaimed waters and natural waters, BRO has a rigid molecular structure and is usually toxic to microorganisms (Wang et al. 2018). And the biodegradation rate (BOD/COD) of BRO is usually lower than 0.2 (Desheng et al. 2013).

First author: Zhifeng Hu

Responsible editor: Bingcai Pan

Electronic supplementary material The online version of this article (https://doi.org/10.1007/s11356-018-3919-5) contains supplementary material, which is available to authorized users.

✉ Desheng Li
dsli@bjtu.edu.cn

Zhifeng Hu
zhifenghu@bjtu.edu.cn

[1] School of Civil Engineering, Beijing Jiaotong University, Beijing 100044, China

[2] Key Laboratory of Aqueous Typical Pollutants Control and Water Quality Safeguard, Beijing 100044, People's Republic of China

Therefore, biological processes are not applicable to both NO_3^-–N removal and BRO degradation in reclaimed water. Thus, it is necessary to develop technologies of simultaneous nitrate and biorefractory organics removal. Xu et al. (2018) found that the removal of DOM and nitrate from WWTP effluents using photocatalytic membranes is an advanced approach for the treatment of secondary effluent. Feng et al. (2015) found that the microbial fuel cell technology holds potential for simultaneous removal of phenolic compounds and nitrogen contained in some particular industrial wastewaters. Zhang et al. (2018) offered a self-sustaining approach based on catalytic reactions of hydroxyl and chlorine radicals for simultaneous nitrogen-containing organic wastewater treatment and electricity production.

Over the past two decades, the chemical reduction of NO_3^-–N utilizing zero-valent iron (ZVI) as a reducing agent (electron donor) has been widely studied due to its high efficiency for NO_3^-–N removal without the consumption of organic carbon sources (Hwang et al. 2015; Tang et al. 2013). However, results have shown that NO_3^-–N is only effectively reduced by ZVI under strong acid conditions (pH 2.0~4.0) due to the formation of iron (hydr)oxides on the surface of ZVI (Tang et al. 2013). Moreover, the main product of ZVI-based NO_3^-–N reduction is ammonia (Tang et al. 2013). To decrease the strong inhibitory effect of pH on NO_3^-–N reduction by ZVI, nanoscale zero-valent iron (nZVI) was developed and applied to NO_3^-–N reduction (Schmidt and Clark 2012; Westerhoff and James 2003). The specific surface area and physicochemical activity of nZVI represent a dramatic improvement relative to the properties of ZVI (Shi et al. 2018). Substantial research has shown that a NO_3^-–N removal efficiency of 95–100% can be achieved under neutral conditions by nZVI (Hwang et al. 2015). Nevertheless, the extremely high cost of nZVI production, accumulation of undesirable ammonia, and rapid passivation of nZVI in water have made nZVI unsuitable for practical use (Hwang et al. 2015; Kiskira et al. 2017). Therefore, further investigations on the applicability of ZVI-based NO_3^-–N reduction are required.

Our previous study showed that iron-carbon microelectrolysis (IC-ME) can occur when ZVI is attached to activated carbon (AC), even in neutral or alkali solutions, using ZVI as the anode and AC as the cathode (Deng et al. 2017; Desheng et al. 2015; Li et al. 2013). The supply of electrons from ZVI can be enhanced by IC-ME to generate electrons and Fe^{2+} and Fe^{3+} at the anode, as shown by Eqs. (1)–(2) (Deng et al. 2016b, 2017; Desheng et al. 2015). Then, the newly generated electrons are transferred to the cathode to reduce the oxidizing agent (electron acceptor) adsorbed by the AC (Deng et al. 2016a, 2017; Desheng et al. 2015). Equation (3) shows the reaction when H^+ acts as the electron acceptor (Deng et al. 2016a). Equations (4)–(5) show the reaction when NO_3^-–N acts as the electron acceptor. In solution, NO_3^-–N is predominantly reduced due to its relatively higher oxidation potential (Weast 1989). Additionally, the residual Fe^{2+} at the anode can also be utilized as a reductant for NO_3^-–N reduction under acidic conditions, as Eq. (6) shows (Kiskira et al. 2017; Weast 1989). In our application of iron scraps (ISs, scrap iron from mechanical processing factories) and AC-based IC-ME (Desheng et al. 2015), the reduction rate of NO_3^-–N improved from 23 g NO_3^-–N $(m^3 \cdot d)^{-1}$ (when using ISs as a reducing agent) to 81 g NO_3^-–N $(m^3 \square d)^{-1}$ at an influent pH of 6.5–7.0 with an increase in the reaction rate constant from 0.11×10^{-4} to 0.39×10^{-4}, as calculated via the third-order kinetics equation. The application of IC-ME dramatically improved the efficiency of ZVI-based NO_3^-–N reduction, which also promotes the reuse of ISs for nitrogen removal.

$$Fe \rightarrow Fe^{2+} + 2e; E^0\left(Fe^{2+}/Fe\right) = -0.44\ V \quad (1)$$

$$Fe^{2+} \rightarrow Fe^{3+} + e; E^0\left(Fe^{3+}/Fe^{2+}\right) = -0.77\ V \quad (2)$$

$$2H^+ + 2e \rightarrow 2[H] \rightarrow H_2; E^0(H^+/H_2) = 0\ V \quad (3)$$

$$NO_3^- + 5e + 3H_2O \rightarrow 0.5N_2 + 6OH^-; E^0(NO_3^-/N_2) > 0\ (\textit{Depending on the reduction pathways.}) \quad (4)$$

$$NO_3^- + 8e + 7H_2O \rightarrow NH_4^+ + 10OH^-; E^0(NO_3^-/NH_4^+) > 0\ (\textit{Depends on the reduction pathways}) \quad (5)$$

$$NO_3^- + (8-6n)Fe^{2+} + 6H^+ \rightarrow nN_2 + (1-2n)NH_4^+ + (8-6n)Fe^{3+} + 3H_2O \quad (6)$$

However, after secondary biotreatment, the pH of real reclaimed water is higher than 7.0 and usually near 8.5 ± 0.5 (Metcalf and Eddy 2004). Thus, the pH required (6.5~7.0) for IC-ME-based NO_3^-–N reduction is not applicable for practical reclaimed water treatment. Moreover, a considerable amount of ammonia is still produced in IC-ME-based NO_3^-–N reduction, although the amount is much lower than that produced by ZVI-based NO_3^-–N reduction (Desheng et al. 2015; Xing et al. 2016). Therefore, further research should be conducted to improve the NO_3^-–N reduction rate of IC-ME and simultaneously reduce ammonia production.

Many previous studies have shown that the ZVI-based redox reaction can be catalyzed by certain metal catalysts. Devi and Saroha (2015) found that the reduction efficiency of pentachlorophenol by ZVI was dramatically enhanced when palladium (Pd) was attached to ZVI to form Pd/Fe bimetallic nanoparticles. Lubphoo et al. (2015) investigated the enhancement of NO_3^-–N reduction by ZVI upon adding copper (Cu) and Pd. Their research found that the reaction rate was sustainably improved by both Cu and Pd and that an increase in the Pd addition could suppress the formation of ammonia (Lubphoo et al. 2015). Deng et al. (2017) utilized manganese

(Mn) and nickel (Ni) to enhance IC-ME-based phosphonate adsorption and found that the addition of Mn and Ni both significantly promoted the dissolution of Fe^{3+} from ISs.

Thus, in the present study, Cu, Mn, Ni, and Pd were mixed together as a composite catalyst (CC) for IC-ME-based NO_3^-–N reduction to improve the reduction efficiency at high pH and simultaneously reduce ammonia production.

Moreover, degradation of resident BRO is a common problem (Wang et al. 2018). Some other studies have reported the BRO degradation ability of microelectrolysis (Ying et al. 2012; Zhou et al. 2013). Microelectrolysis is widely used in industrial organic wastewater treatment, such as coking wastewater treatment, because of its low cost, convenient operation, and high efficiency (Qin et al. 2012). Nevertheless, the application of microelectrolysis for simultaneous NO_3^-–N reduction and BRO degradation has not been investigated.

Thus, in the present study, an IS- and AC-based catalyzed IC-ME carrier was prepared, and the removal performance of NO_3^-–N and BRO in reclaimed water by IC-ME and catalyzed IC-ME was investigated. The enhancement derived from CC addition and the impact of pH and external AC addition on NO_3^-–N reduction and BRO degradation by IC-ME were studied. Then, the NO_3^-–N reduction kinetics and BRO degradation mechanism in the presence of catalyzed IC-ME were analyzed. This work aimed to provide an applicable technology and corresponding theoretical basis for simultaneous advanced removal of NO_3^-–N and resident COD from reclaimed water. This research could also provide an approach for IS reuse in wastewater treatment.

Materials and methods

Preparation of IC-ME

Raw materials, including ISs, AC, CC (consisting of Cu, Mn, Ni, and Pd, as mentioned in the "Introduction" section), adhesive X, and foaming agent Y, were used in the preparation of the catalyzed IC-ME system. The ISs (10~20 mesh) were purchased from a metal processing factory (Gongyi Metal Processing Factory, Gongyi City, China). AC (200 mesh), Cu (> 99%, 300 mesh), Mn (> 99%, 300 mesh), Ni (> 99%, 300 mesh), Pd (> 99%, 300 mesh), adhesive X (> 99%, dissoluble), and foaming agent Y (> 99%, dissoluble) were purchased from Beijing Chemical Reagent Factory (Beijing, China). The CC was initially prepared at a Cu:Mn:Ni:Pd volume ratio of 1:1:1:0.5 according to our previous study (Li 2013). For the IC-ME preparation (Fig. 1), ISs and AC were added at a volume ratio of 1.5:1, which was the optimal volume ratio for microelectrolysis that was calculated in our previous research (Deng et al. 2017); then, a certain volume (calculated in the present research) of CC was added. Finally, the obtained IC-ME was ground to 15~20 mesh and set aside.

Synthetic reclaimed water

Synthetic reclaimed water was prepared to simulate real effluent of secondary biotreatment from WWTP in accordance with Standard A of the First Class in "Chinese Discharge Standard of Pollutants for Municipal Wastewater Treatment Plant (GB18918-2002)." Meanwhile, the concentration of NO_3^-–N and COD of synthetic reclaimed water was increased appropriately. On the account that advanced removal of NO_3^-–N and degradation of BRO is imperative in this study and some other pollutants, like suspended solids (SS), are in low concentrations after secondary treatment of WWTP, the main water quality indexes consist of NH_4^+–N, NO_3^-–N, P, and COD for the prepared synthetic reclaimed water are shown in Table 1. NH_4^+–N was added as ammonium chloride (NH_4Cl), NO_3^-–N was added as potassium nitrate (KNO_3) and P was added as monopotassium phosphate (KH_2PO_4). To simulate the low biodegradability of reclaimed water (BOD/COD < 0.2), COD was added as humic acid and glucose ($C_6H_{12}O_6$). All the reagents mentioned above were purchased from Beijing Chemical Reagent Factory.

Experimental procedures

Jar tests were designed to examine the NO_3^-–N reduction and BRO degradation performance of the catalyzed IC-ME, as well as the impact of the pH and external AC addition. The experimental setup is shown in Fig. 2. The reactor, a 500-mL beaker, was placed on a retort stand. An electronic blender (MYP2011, Hijiu, Shanghai, China) was set in the beaker for mixing, and the speed was controlled at 180 r/min with a speed regulator (MYP2011-1, Hijiu, Shanghai, China). A temperature regulator (FY 500, Fengyi, Zhejiang, China) was used to control the reaction temperature.

The effects of the CC, external AC addition, and pH on the reduction efficiency were separately explored. Thus, three groups were included in the experiment (Table 2). The enhancement effect of CC addition (0, 5, 10, 15 μL mL^{-1} IC-ME) on nitrate reduction and BRO removal of IC-ME was investigated in group 1. Different volumes of external AC (0, 2.5, 5.0, 7.5 mL L^{-1} reclaimed water) were added in group 2. In group 3, the pH was controlled at 3.0 ± 0.1, 7.0 ± 0.1, and 8.5 ± 0.1 using a hydrochloric acid (HCl) solution (1 mol L^{-1}) or sodium hydroxide (NaOH) solution (10%). A pH of 8.5 was chosen in this study because the pH of practical reclaimed water is higher than 7.0 and usually near 8.5 ± 0.5(Metcalf and Eddy 2004). The ground IC-ME ("Preparation of IC-ME" section) dosage was controlled at 40 mL L^{-1}. The temperature in the reaction solutions was kept at 25 ± 1 °C.

Samples with a volume of 5 mL were collected at 10 min, 30 min, 60 min, 120 min, 180 min, 240 min, 360 min, and 480 min. The pH and oxygen reduction potential (ORP) in the reactor were recorded by a pH electrode (6, pHG_7685A,

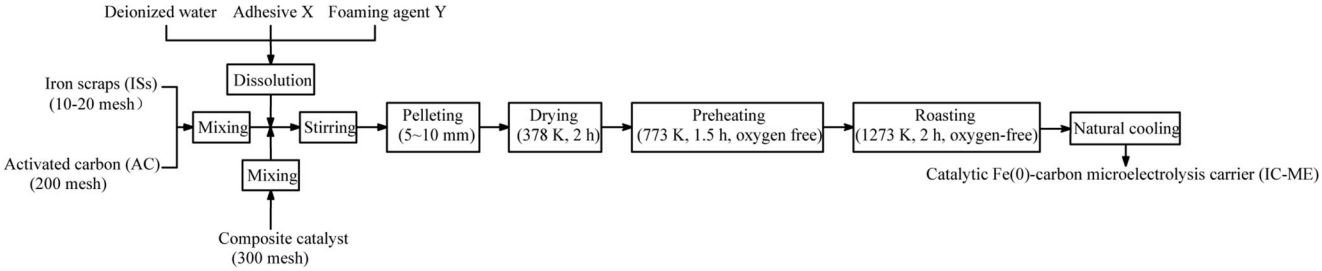

Fig. 1 The process of IC-ME preparation

LEICI, Shanghai, China) and ORP meter (SG2-T, Mettler Toledo, Switzerland), respectively. The samples were filtered through a 0.45-μm membrane filter immediately after sampling, and COD, NH_4^+–N, NO_3^-–N, and NO_2^-–N were detected.

Analytical methods

The concentrations of NH_4^+–N, NO_3^-N, and NO_2^-–N were determined using an ultraviolet-visible (UV-Vis) spectrophotometer (TU 1810, Purkinje, China) according to "Water and Wastewater Monitoring and Analysis Methods" (Chinese State Environmental Protection Administration). Specifically, NH_4^+–N, NO_3^-–N, and NO_2^-–N were detected via Nessler's reagent spectrophotometry, UV spectrophotometry, and *N*-(1-naphthyl)-ethylenediamine dihydrochloride spectrophotometry, respectively. Total nitrogen (TN) was calculated as the sum of the NO_3^-–N, NH_4^+–N, and NO_2^-–N concentrations. COD was determined using a COD analyzer (COD Max II, Hach Co. Ltd., USA). The pH and ORP were measured using the methods introduced in the "Experimental procedures" section.

Results and discussion

The enhancement effect of CC on nitrate reduction and BRO removal by IC-ME

Figure 3 shows the effect of CC addition on nitrate reduction and BRO degradation by IC-ME. Nitrate was reduced, as shown in Fig. 3a. The NO_3^-–N reduction efficiency of the catalyzed IC-ME was higher than that of the IC-ME. The reduction efficiency of NO_3^-–N in all three catalyzed systems reached 30% at 10 min, while only a 2.7% reduction efficiency was obtained in the absence of CC. Additionally, the NO_3^-–N reduction rate increased with the increase in the CC addition. Nitrate was substantially reduced by 97.8% after 240 min with a CC/IC-ME volume ratio of 15 μL mL^{-1}. Figure 3b shows that NH_4^+–N gradually increased with the reaction time in the IC-ME-based NO_3^-–N reduction system. In contrast, with an increase in the CC addition, an increase in the NH_4^+–N concentration was no longer observed; instead, the NH_4^+–N in the influent was effectively removed. When the CC/IC-ME volume ratio reached 15 μL mL^{-1}, the NH_4^+–N removal efficiency reached 43.6% in 240 min.

According to the research of (Luo et al. 2014), NO_3^-–N reduction can be enhanced by Fe(0)-carbon microelectrolysis. The research of Devi and Saroha (2015) showed that the addition of certain catalysts can increase the NO_3^-–N reduction rate. Similarly, the CC addition substantially enhanced nitrate reduction in the present research, and the reduction efficiency increased with the increasing CC addition. According to the research of (Luo et al. 2014), NH_4^+–N increases because NO_3^-–N is reduced to NH_4^+–N by IC-ME. The research of Devi and Saroha (2015) showed that a single catalyst cannot suppress the formation of NH_4^+–N. In particular, in this study, the CC addition dramatically inhibited ammonia production.

The research of Yang et al. (2017) confirmed BRO removal by IC-ME. The COD removal mechanism in the IC-ME system consists of the following two steps: (1) Fe(0)-carbon microelectrolysis (Li et al. 2017) and (2) AC adsorption (Desheng et al. 2013). The process can (1) break the chains of BRO and transform the material into small-molecule organic compounds. Small-molecule organic compounds are much more easily adsorbed by AC during the process. (2) As Fig. 3d shows, IS- and AC-based IC-ME also showed similar effects. Moreover, Fig. 3c also shows that the addition of CC accelerated the removal of COD in the IC-ME system. The removal rate of COD reached 42.5~58.8% after 10 min when CC was added to the IC-ME system. However, the increase in the CC addition yielded little improvement in BRO removal. Since no additional AC was added to the system, the adsorption capacity did not increase. The reason for the improvement in BRO removal efficiency was

Table 1 Characteristics of the synthetic reclaimed water

Parameter	COD (mg·L^{-1})	NH_4^+–N (mg·L^{-1})	NO_3^-–N (mg·L^{-1})	TN (mg·L^{-1})
Synthetic reclaimed water	78.86~80.05	5.01~5.41	14.93~15.61	19.94~20.64
GB 18918-2002	80	5	15	20

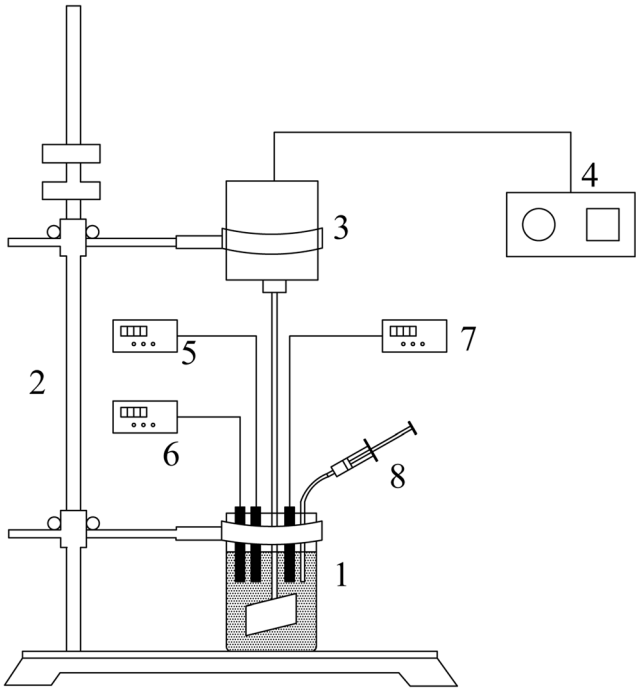

Fig. 2 Schematic diagram of the experimental setup. 1, Beaker; 2, Retort stand; 3, Speed regulator; 4, Electronic blender; 5, Temperature regulator; 6, pH electrode; 7, ORP meter; 8, Sampler (syringe)

that the catalytic Fe(0)/AC microelectrolysis process could break the chains of BRO and transform the material into small-molecule organic compounds, which were much more easily adsorbed by AC. Furthermore, metal ions (such as Cu^{2+}, Ni^{2+}) on the effluent were measured and no metal ion (except Fe^{2+} and Fe^{3+}) was found in the effluent, which would not cause secondary pollution to treated water quality.

Effect of external AC addition on the performance of catalyzed IC-ME

The results in the "The enhancement effect of CC on nitrate reduction and BRO removal by IC-ME" section show that the addition of CC dramatically improved the BRO removal in reclaimed water due to the improvement of BRO degradation by CC, but an increase in the CC addition yielded little improvement in BRO removal (as in the "The enhancement effect of CC on nitrate reduction and BRO removal by IC-ME" section). Therefore, experiments were conducted to investigate the effect of an external AC addition on BRO removal by catalyzed IC-ME. The results are shown in Fig. 4.

Figure 4a and b shows that an external AC addition had no obvious effect on the removal of NO_3^-–N, which means that IC-ME removed nitrate by chemical reduction rather than physical adsorption. The NH_4^+–N removal efficiency without an external AC addition was 53.5%, whereas the efficiency with an external AC addition of 7.5 mL L^{-1} reclaimed water was 64.3%. An external AC addition increased ammonia removal, but only by 10.8%, which shows that the catalyst must be present initially instead of adding external AC.

Figure 4c shows that with an increase in the external AC addition, the COD removal increased significantly. When the external AC addition was 7.5 mL L^{-1} reclaimed water, the COD removal efficiency reached 53.7% after 10 min and 80.5% after 240 min. The COD removal efficiency was high in the initial reaction, mainly due to reactive oxygen (·O) released by the reaction of the Fe(0)/AC cell, which can transform BRO into small-molecule organic compounds to improve the adsorption efficiency of AC (Yang et al. 2017). The COD removal efficiency decreased gradually in the later stages of the reaction, mainly because the adsorption sites on the surface of AC were gradually occupied, and the adsorption capacity of AC decreased gradually (Desheng et al. 2013). Figure 4d examines the relationship between the COD removal and AC addition. The increase in the AC addition was roughly linear with the increase in the COD removal. Thus, the results of the present study show that CC addition can not only promote the production of O· to promote the degradation of BRO into small-molecule organic compounds but also accelerate the reaction rate. The addition of AC can increase the number of active sites and enhance the ability of IC-ME to adsorb COD. The positive, linear correlation between COD removal and AC addition is fitted in Fig. 4d with $R^2 = 0.85$. This correlation indicates that COD in the reaction system is rarely oxidized to CO_2 by IC-ME and that the removal of COD mainly depends on adsorption by AC.

Effect of pH on the performance of catalyzed IC-ME

pH is an important factor that affects ZVI-based nitrate reduction because this reduction is a hydrogen ion (H^+)-consuming reaction (Liu et al. 2014; Zhang et al. 2017). The obvious

Table 2 Three designed group experiments

Group	IC-ME dosage (mL·L^{-1} reclaimed water)	CC added to IC-ME (μL·mL^{-1} IC-ME)	External AC addition (mL·L^{-1} reclaimed water)	Influent pH
Group 1	20	0, 5, 10, 15	0	7.0 ± 0.1
Group 2	20	15	0, 2.5, 5.0, 7.5	7.0 ± 0.1
Group 3	20	15	7.5	3.0 ± 0.1, 7.0 ± 0.1, 8.5 ± 0.1

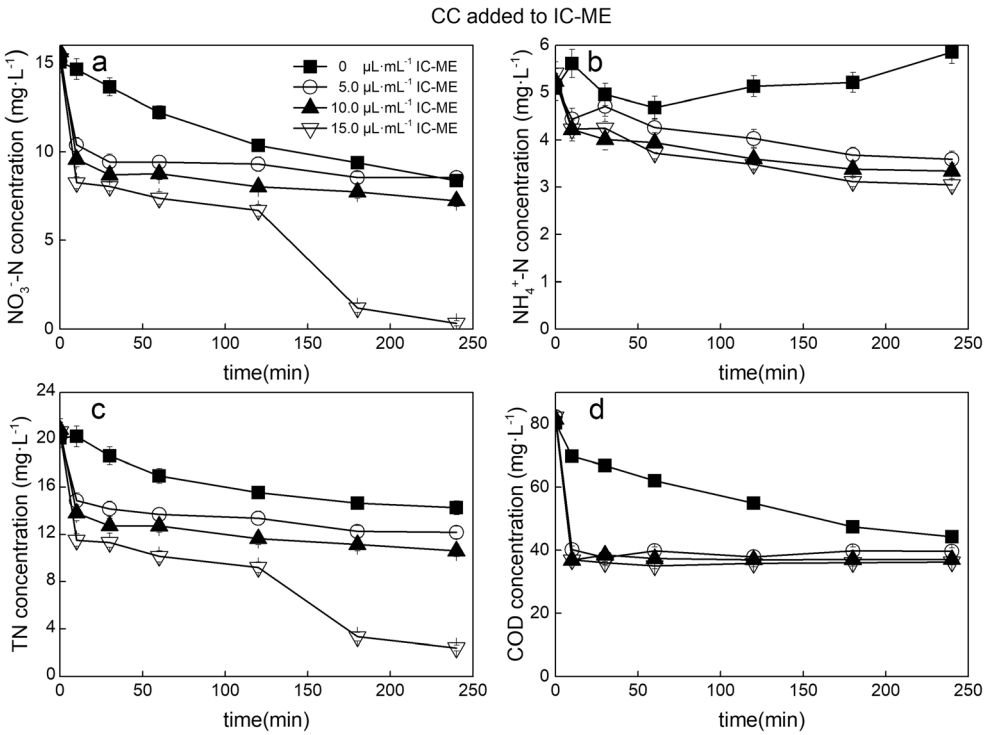

Fig. 3 Effect of CC addition on nitrate reduction and BRO removal by IC-ME. **a** Nitrate; **b** ammonia; **c** total nitrogen; **d** COD

influence of pH on nitrate reduction by IC-ME was also observed in our previous study (Deng et al. 2016a; Desheng et al. 2015). Thus, in the present study, the effect of pH on nitrate reduction by catalyzed IC-ME was also investigated, and the results were compared with those for nitrate reduction by IC-ME and ZVI. The results are shown in Fig. 5.

As shown in Fig. 5a, when the pH was 3.0 ± 0.1, the removal efficiency of NO_3^-–N was the highest and reached 100% after 240 min. With the increase in pH, the NO_3^-–N removal efficiency of the IC-ME decreased, but the reduction efficiency of NO_3^-–N still reached 96.9% at pH = 8.5 ± 0.1. However, as shown in Fig. 5b, 33.2% of the NO_3^-–N was

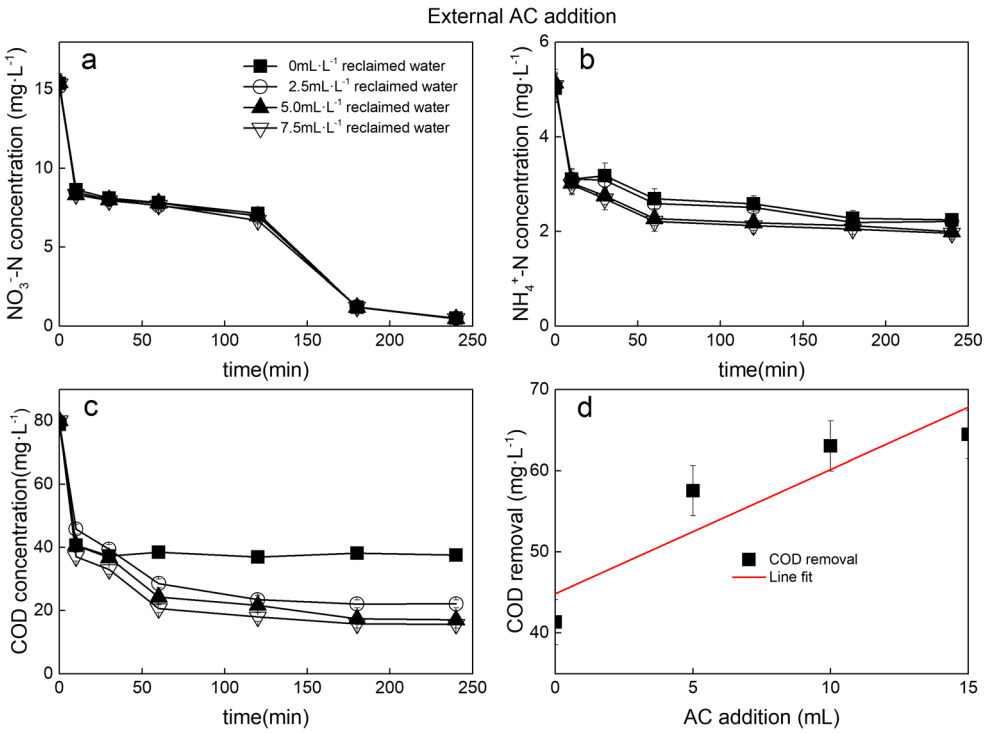

Fig. 4 Effect of external AC addition on the performance of catalyzed IC-ME. **a** Nitrate; **b** ammonia; **c** COD; **d** relationship between COD removal and AC addition

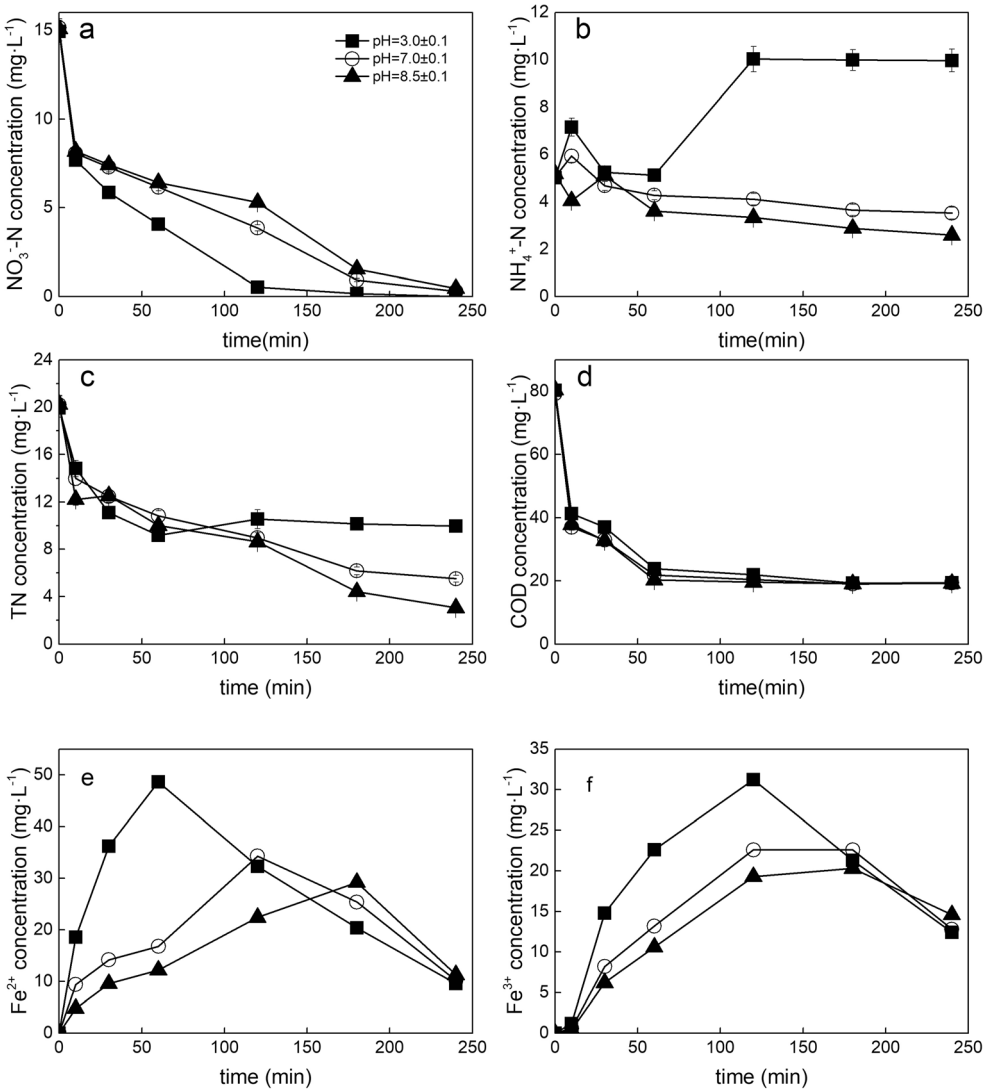

Fig. 5 Effect of pH on the performance of catalyzed IC-ME. **a** Nitrate; **b** ammonia; **c** total nitrogen; **d** COD; **e** Fe^{2+}; **f** Fe^{3+}

converted to NH_4^+–N at pH 3.0 ± 0.1, which cannot result in TN removal. When the pH was 7.0 ± 0.1, NH_4^+–N did not increase substantially, and the NO_3^-–N removal efficiency reached 99.9%. Not only was the NO_3^-–N removed by catalytic microelectrolysis not converted to NH_4^+–N at pH 8.5 ± 0.1, but NH_4^+–N removal was achieved with a removal efficiency of 31.7% after 240 min. Additionally, NO_3^-–N was removed to a level below 0.5 mg L^{-1}. When the pH increased, the reduction potential of NO_3^-–N was reduced, and the reduction product was N_2 or another form of gaseous nitrogen instead of NH_4^+–N. Therefore, the accumulation of NH_4^+–N can be inhibited at high pH (Kiskira et al. 2017; Weast 1989). The NO_3^-–N reduction efficiency and NH_4^+–N accumulation by ZVI, nZVI, IC-ME (including (ZVI-AC)-ME in our previous research and (IS-AC)-ME in the present research), and catalyzed (IS-AC)-ME in the present study were compared and analyzed, and the results are shown in Table 3. Comparing the performances of (IS-AC)-ME and catalyzed (IS-AC)-ME shows that NH_4^+–N is controlled by high pH, while the contribution of CC ensures the reaction rate of IC-ME at high pH.

Figure 5d shows that the removal efficiency of BRO did not have obvious changes under different pH conditions. The results indicated that pH has little effect on BRO removal. However, previous studies have shown that the removal of organic compounds by Fe-carbon microelectrolysis under acidic conditions is much higher (Yang et al. 2017). These varying results indicate that the IC-ME system mainly acts by degrading BRO into small-molecule organic compounds but has little effect on the removal of organics in general. Adsorption by added AC plays the main role in COD removal. Thus, in an IC-ME system, the organic matter can be effectively removed by adding AC instead of adjusting the pH. Moreover, AC addition is a much more practical method than pH adjustment.

Table 3 Comparison of the NO_3^-–N reduction and NH_4^+–N production of Fe-based substrates

Fe-based substrate		pH	NO_3^-–N reduction (%)[a]	NH_4^+–N production (%)[b]	Reference
ZVI		2	40~45	24~28	Rodríguez-Maroto et al. (2009)
		3	6~10	4~8	
ZVI		7	36~44	34~42	Song et al. (2017)
ZVI		1.5	90~96	89~95	Zhang et al. (2017)
nZVI		7	45~50	35~39	Ahn et al. (2008)
IC-ME	ZVI-AC	2	86~92	–	Luo et al. (2014)
		3	66~72	55~61	
		6	6~10	–	
	ISs-AC	7.0 ± 0.1	37.7	0.8	Present research
Catalyzed IS-AC		3.0 ± 0.1	98.9	33.3	Present research
		7.0 ± 0.1	93.9	1.3	
		8.0 ± 0.1	89.8	− 15.3	

[a] Calculated from the present research and the corresponding references by 100% × (NO_3^-–N concentration at 180 min/NO_3^-–N concentration in the influent)

[b] Calculated from the present research and the corresponding references by 100% × (NH_4^+–N concentration at 180 min/NO_3^-–N concentration in the influent)

Figure 5e and f shows the concentration of Fe^{2+} and Fe^{3+} in the solution. Obviously, the lower the pH, the more Fe^{2+} and Fe^{3+} were produced and the faster the generation rate. The Fe^{2+} was generated to the maximum concentration of 48.6 mg L^{-1} in 60 min, 34.3 mg L^{-1} in 120 min, and 29.2 mg L^{-1} in 180 min at initial pH 3.0 ± 0.1, 7.0 ± 0.1, and 8.5 ± 0.1, respectively. Similarly, the Fe^{3+} was generated to the maximum concentration of 31.2 mg L^{-1} in 120 min, 22.6 mg L^{-1} in 120 min, and 20.3 mg L^{-1} in 180 min at initial pH 3.0 ± 0.1, 7.0 ± 0.1, and 8.5 ± 0.1, respectively. Fe^{2+} and Fe^{3+} were produced in all the reaction times, and the pH of the solution is higher than the initial, and the precipitation occurred at all the reaction times. The Fe^{2+} and Fe^{3+} were almost totally precipitated from the maximum concentration to a low concentration in the last 120 min. Thus, the generation and precipitation of Fe^{2+} and Fe^{3+} in this system is a dynamic process; in the first 120 min, the effect of generation is dominant; while in the last 120 min, the precipitation of Fe^{2+} and Fe^{3+} becomes dominant.

Kinetics evaluation and mechanism analysis on catalyzed IC-ME-based advanced reclaimed water treatment

Kinetic evaluation of nitrate reduction by catalyzed IC-ME

The time-dependent variations in nitrate and BRO in reclaimed water treated by catalyzed IC-ME with a CC/IC-ME volume ratio of 15 μL mL^{-1}, AC addition of 7.5 mL mL^{-1} catalyzed IC-ME, and pH of 7.0 ± 0.1 are shown in Fig. 5a and b. To further ascertain the removal rate of nitrate and BRO in reclaimed water, the kinetics of nitrate reduction and BRO degradation by catalyzed IC-ME were evaluated.

Linear regression was used to explore the kinetics of NO_3^-–N and COD removal from reclaimed water in the IC-ME system. The equation for the degradation rate of NO_3^-–N and COD was established as (7).

$$v = kC^n \tag{7}$$

where v is the reaction rate, milligrams per liter per minute; k is the reaction rate constant; and n is the reaction order.

The concentration of pollutants in the solution at reaction time t is given as (8):

$$C_t = C_0 - vt = C_0 - tkC^n \tag{8}$$

where C_t is the residual concentration of pollutants at time t, milligrams per liter; and C_0 is the initial concentration of pollutants, milligrams per liter.

The data were plotted against time, t, as $-\ln(C_t/C_0)$, $(1/C_t - 1/C_0)$, and $0.5(1/C_t^2 - 1/C_0^2)$ using regression for the first-, second-, and third-order reaction kinetics equations to calculate the correlation coefficients. The test results and linear relationship coefficients for nitrate removal by IS-AC and catalyzed IC-ME are shown in Fig. 6a, b, c and Supplementary Material, respectively.

Under the action of catalytic IC-ME, the reaction rate constant of NO_3^-–N reduction is an order of magnitude higher than that of IS-AC under neutral conditions. This result indicates that in the catalyzed IS-AC system, the addition of CC enhances the mass transfer of nitrate from the solution to the iron surface, which accelerates the rate of nitrate reduction and verifies the conclusion in the "The Enhancement Effect of CC on nitrate reduction and BRO removal by IC-ME" section.

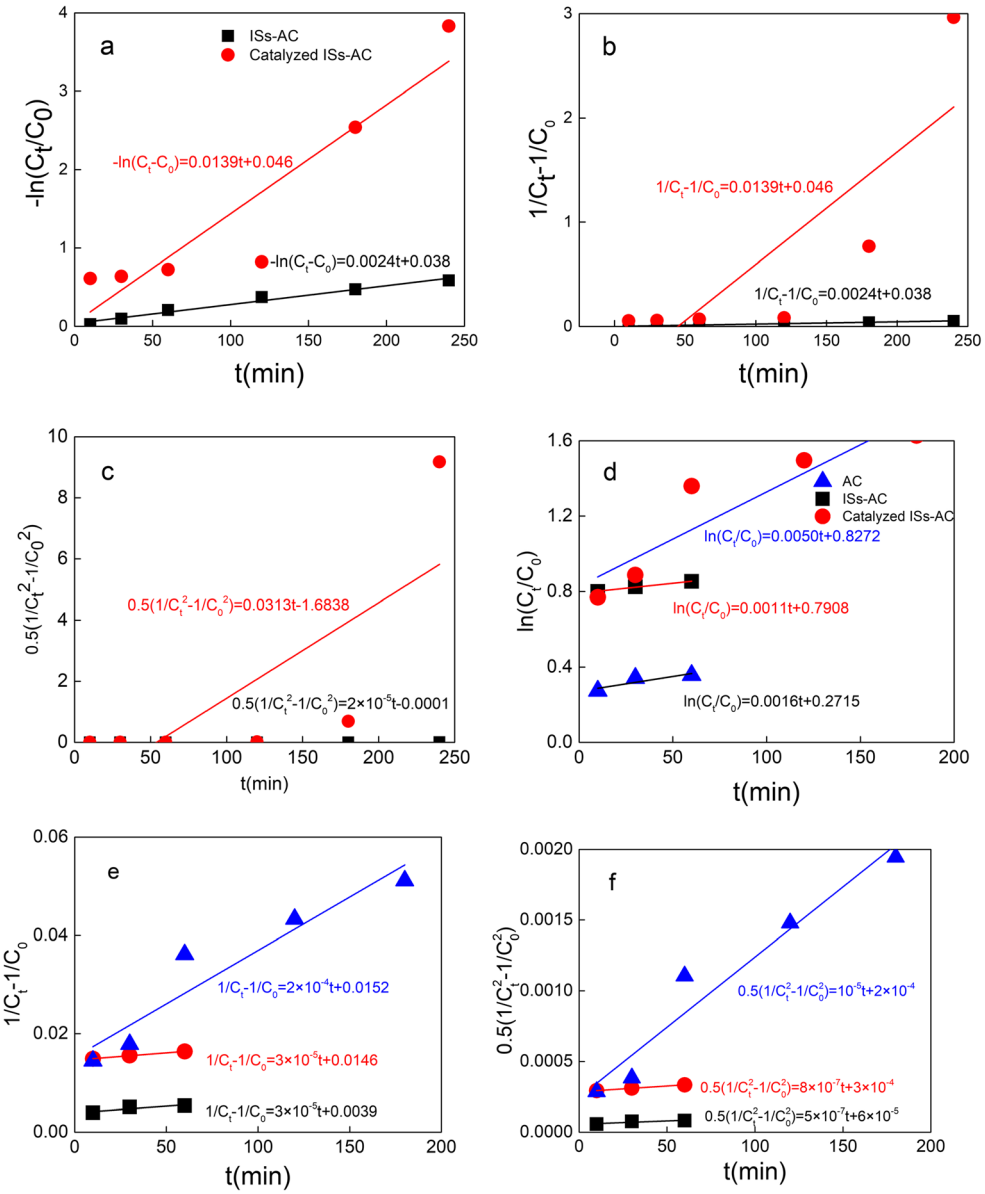

Fig. 6 Linear regression analysis of nitrate reduction and COD removal by IS-AC and catalyzed IS-AC modeled with different reaction orders. **a** First-order reaction of nitrate; **b** second-order reaction of nitrate; **c** third-order reaction of nitrate; **d** first-order reaction of COD; **e** second-order reaction of COD; **f** third-order reaction of COD

Kinetic evaluation of BRO degradation by catalyzed IC-ME

Figure 6d, e, f and the Supplementary Material show the correlation coefficients of AC, IS-AC, and catalyzed IS-AC for COD reduction. The kinetic reaction of BRO degradation with AC, IS-AC, and catalyzed IS-AC was fitted by the third-order-reaction kinetic equation. The reaction rate of BRO degradation by catalyzed IS-AC was two orders of magnitude greater than that generated by AC and IS-AC. The [H] and O· generated by Fe(0)–C microelectrolysis destroy the carbon chains in BRO, reduce the molecular weight of organic compounds, and promote the adsorption and removal of organic compounds by AC. Moreover, the addition of CC enhances the reaction rate of BRO degradation, augments the effect of Fe(0)–C microelectrolysis, and improves the chemical activity of [H] and O·.

Mechanistic analysis of the catalyzed IC-ME-based advanced reclaimed water treatment

Figure 7 shows a proposed mechanism of the effect of IC-ME on nitrate reduction and BRO degradation. ISs and AC, which have an electrode potential difference of approximately 1.2 V, are porous materials with a high adsorption capacity. When Fe (anode) and AC (cathode) are mixed and come into contact in reclaimed water, a large number of microcells are spontaneously formed in the IC-ME system, and electrons are produced in the anode and transferred to the cathode. The adsorbed H^+ or H_2O molecules on the AC surface accept the electrons, are converted into adsorbed [H], and then rapidly reduce the neighboring adsorbed NO_3^-–N to N_2 and NH_4^+–N. The Fe^{2+} generated at the anode and the [H] and O· generated at the cathode

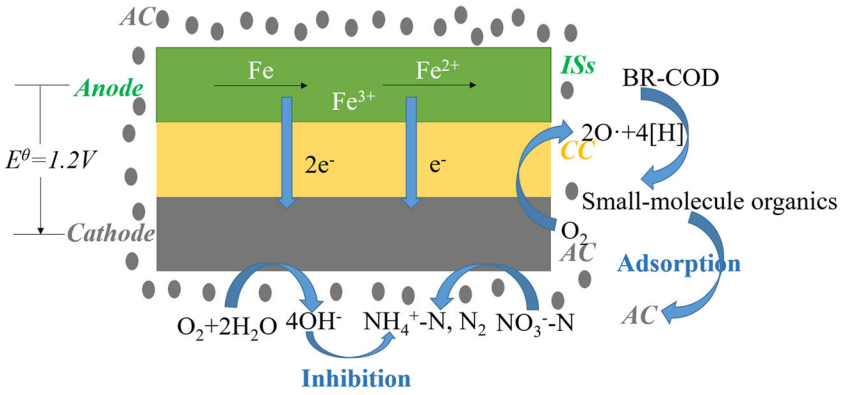

Fig. 7 Proposed mechanism of IC-ME for nitrate reduction and BRO degradation

have strong chemical activities and can effectively destroy the carbon chains in organic contaminants and mineralize the contaminants into small-molecule organic compounds. The added AC can adsorb these small-molecule organic compounds.

Possibility of reusing ISs for advanced reclaimed water treatment

The catalyzed IC-ME system shows great performance for nitrate reduction and BRO degradation even though the purity of ISs is low compared with that of ZVI and nZVI. With the addition of CC, nitrate and BRO can be removed under neutral or alkaline conditions. The application of catalyzed IS-AC removes the pH reliance of ZVI and Fe(0)-C microelectrolysis and inhibits the generation of ammonia. The main consumables in the proposed IC-ME process, ISs, are produced worldwide, especially in industrialized countries. Large amounts of capital are being invested and massive quantities of energy are being consumed to recover ISs from steel mills (Hongbiao et al. 2016), resulting in the low price of ISs (almost one third of the cost of ZVI) (Alessio 2015; Hongbiao et al. 2016). Given its practical benefits, including no security risk, low capital and operational costs, and simple operational procedure, the catalyzed IC-ME process shows great potential for full-scale applications for simultaneous nitrate reduction and BRO degradation in reclaimed water.

Conclusions

Nitrate reduction and BRO degradation in reclaimed water by catalyzed IC-ME were investigated. The results support the following conclusions:

- The IC-ME system was investigated for effective nitrate reduction in aqueous solution at pH values from 3.0 to 8.5.
- The study showed that the IC-ME system reduced nitrate in neutral and alkaline conditions with a reduction efficiency of up to 96%, which depended on the volume of CC added.
- Fe(0)-carbon microelectrolysis in the IC-ME system oxidized BRO into small-molecule organic compounds, and AC addition enhanced the reduction efficiency of organics in aqueous solution.

The IC-ME system has thus shown great potential for application in nitrate and BRO reduction in reclaimed water owing to its high efficiency and cost-effectiveness in a wide pH range.

Funding information This work was supported by the Fundamental Research Funds for the Central Universities (No. 2018YJS123) and the National Natural Science Foundation of China (No. 51778040).

References

Ahn SC, Oh SY, Cha DK (2008) Enhanced reduction of nitrate by zero-valent iron at elevated temperatures. J Hazard Mater 156:17–22. https://doi.org/10.1016/j.jhazmat.2007.11.104

xAlessio S (2015) Use of nanoscale zero-valent iron (NZVI) particles for chemical denitrification under different operating conditions. Metals 5:1507–1519

Chen J, Liu S, Yan J, Wen J, Hu Y, Zhang W (2017) Intensive removal efficiency and mechanisms of carbon and ammonium in municipal wastewater treatment plant tail water by ozone oyster shells fix-bed bioreactor − membrane bioreactor combined system. Ecol Eng 101: 75–83. https://doi.org/10.1016/j.ecoleng.2016.11.029

Cho D-W, Chon C-M, Jeon B-H, Kim Y, Khan MA, Song H (2010) The role of clay minerals in the reduction of nitrate in groundwater by zero-valent iron. Chemosphere 81:611–616. https://doi.org/10.1016/j.chemosphere.2010.08.005

Deng S, Li D, Yang X, Xing W, Li J, Zhang Q (2016a) Biological denitrification process based on the Fe(0)–carbon micro-electrolysis for simultaneous ammonia and nitrate removal from low organic carbon water under a microaerobic condition. Bioresour Technol 219:677–686. https://doi.org/10.1016/j.biortech.2016.08.014

Deng S, Li D, Yang X, Zhu S, Xing W (2016b) Advanced low carbon-to-nitrogen ratio wastewater treatment by electrochemical and biological coupling process. Environ Sci PollutR Int 23:5361–5373. https://doi.org/10.1007/s11356-015-5711-0

Deng S, Li D, Yang X, Xing W, Li J, Zhang Q (2017) Iron [Fe(0)]-rich substrate based on iron–carbon micro–electrolysis for phosphorus adsorption in aqueous solutions. Chemosphere 168:1486–1493. https://doi.org/10.1016/j.chemosphere.2016.11.043

Desheng L, Taixing F, Yanbing S, Weizhong W (2013) Electrochemical technology for denitrification of tail water from wastewater treatment plant. CIESC J (China) 64:1084–1090

Desheng L, Qianyi H, Yuwei C, Shihai D (2015) Chemical catalytic performance on nitrate removal of simulated groundwater. CIESC J (China) 66:2288–2294

Devi P, Saroha AK (2015) Simultaneous adsorption and dechlorination of pentachlorophenol from effluent by Ni–ZVI magnetic biochar composites synthesized from paper mill sludge. Chem Eng J 271:195–203. https://doi.org/10.1016/j.cej.2015.02.087

Feng C, Huang L, Yu H, Yi X, Wei C (2015) Simultaneous phenol removal, nitrification and denitrification using microbial fuel cell technology. Water Res 76:160–170. https://doi.org/10.1016/j.watres.2015.03.001

Gao L, Zhou W, Huang J, He S, Yan Y, Zhu W, Wu S, Zhang X (2017) Nitrogen removal by the enhanced floating treatment wetlands from the secondary effluent. Bioresour Technol 234:243–252. https://doi.org/10.1016/j.biortech.2017.03.036

He S, Wang Y, Li C, Li Y, Zhou J (2018) The nitrogen removal performance and microbial communities in a two-stage deep sequencing constructed wetland for advanced treatment of secondary effluent. Bioresour Technol 248:82–88. https://doi.org/10.1016/j.biortech.2017.06.150

Hongbiao X, Pengpeng X, Hong X, SHaokun Z, Zhongkai R (2016) Finite element simulation and experiment of composite rolling of stainless steel/iron scrap. J Plasticity Eng (China) 23:69–72

Hwang Y, Mines PD, Jakobsen MH, Andersen HR (2015) Simple colorimetric assay for dehalogenation reactivity of nanoscale zero-valent iron using 4-chlorophenol. Appl Catal B Environ 166-167:18–24. https://doi.org/10.1016/j.apcatb.2014.10.059

Kiskira K, Papirio S, van Hullebusch ED, Esposito G (2017) Fe(II)-mediated autotrophic denitrification: a new bioprocess for iron bioprecipitation/biorecovery and simultaneous treatment of nitrate-containing wastewaters. Int Biodeterior Biodegrad 119:631–648. https://doi.org/10.1016/j.ibiod.2016.09.020

Lee KP, Arnot TC, Mattia D (2011) A review of reverse osmosis membrane materials for desalination—development to date and future potential. J Membr Sci 370:1–22. https://doi.org/10.1016/j.memsci.2010.12.036

Le-Minh N, Khan SJ, Drewes JE, Stuetz RM (2010) Fate of antibiotics during municipal water recycling treatment processes. Water Res 44:4295–4323. https://doi.org/10.1016/j.watres.2010.06.020

Li D (2013) A porous granulated biological carrier for nitrogen removal of low carbon to nitrogen ratio wastewater under aerobic conditions and its preparation processes. China, CN201310093411

Li B, Sun K, Guo Y, Tian J, Xue Y, Sun D (2013) Adsorption kinetics of phenol from water on Fe/AC. Fuel 110:99–106. https://doi.org/10.1016/j.Fuel.2012.10.043

Li P, Liu Z, Wang X, Guo Y, Wang L (2017) Enhanced decolorization of methyl orange in aqueous solution using iron–carbon microelectrolysis activation of sodium persulfate. Chemosphere 180:100–107. https://doi.org/10.1016/j.chemosphere.2017.04.019

Liu Y, Li S, Chen Z, Megharaj M, Naidu R (2014) Influence of zero-valent iron nanoparticles on nitrate removal by Paracoccus sp. Chemosphere 108:426–432. https://doi.org/10.1016/j.chemosphere.2014.02.045

Lubphoo Y, Chyan J-M, Grisdanurak N, Liao C-H (2015) Nitrogen gas selectivity enhancement on nitrate denitrification using nanoscale zero-valent iron supported palladium/copper catalysts. J Taiwan Inst Chem E 57:143–153. https://doi.org/10.1016/j.jtice.2015.05.005

Luo J, Song G, Liu J, Qian G, Xu ZP (2014) Mechanism of enhanced nitrate reduction via micro-electrolysis at the powdered zero-valent iron/activated carbon interface. J Colloid Interface Sci 435:21–25. https://doi.org/10.1016/j.jcis.2014.08.043

Metcalf Eddy I (2004) Wastewater engineering: Treatment, disposal, reuse. McGraw-Hill, New York

Ozgun H, Dereli RK, Ersahin ME, Kinaci C, Spanjers H, van Lier JB (2013) A review of anaerobic membrane bioreactors for municipal wastewater treatment: integration options, limitations and expectations. Sep Purif Technol 118:89–104. https://doi.org/10.1016/j.seppur.2013.06.036

Qin L, Zhang G, Meng Q, Xu L, Lv B (2012) Enhanced MBR by internal micro-electrolysis for degradation of anthraquinone dye wastewater. Chem Eng J 210:575–584. https://doi.org/10.1016/j.cej.2012.09.006

Rodríguez-Maroto JM, García-Herruzo F, García-Rubio A, Gómez-Lahoz C, Vereda-Alonso C (2009) Kinetics of the chemical reduction of nitrate by zero-valent iron. Chemosphere 74:804–809. https://doi.org/10.1016/j.chemosphere.2008.10.020

Schmidt CA, Clark MW (2012) Efficacy of a denitrification wall to treat continuously high nitrate loads. Ecol Eng 42:203–211. https://doi.org/10.1016/j.ecoleng.2012.02.006

Shi D, Zhang X, Wang J, Fan J (2018) Highly reactive and stable nanoscale zero-valent iron prepared within vesicles and its high-performance removal of water pollutants. Appl Catal B Environ 221:610–617. https://doi.org/10.1016/j.apcatb.2017.09.057

Song X, Chen Z, Wang X, Zhang S (2017) Ligand effects on nitrate reduction by zero-valent iron: role of surface complexation. Water Res 114:218–227. https://doi.org/10.1016/j.watres.2017.02.040

Tang S, X-m W, H-w Y, Xie YF (2013) Haloacetic acid removal by sequential zero-valent iron reduction and biologically active carbon degradation. Chemosphere 90:1563–1567. https://doi.org/10.1016/j.Chemosphere.2012.09.046

Wang X, Wang J, Li K, Zhang H, Yang M (2018) Molecular characterization of effluent organic matter in secondary effluent and reclaimed water: comparison to natural organic matter in source water. J Environ Sci 63:140–146. https://doi.org/10.1016/j.jes.2017.03.020

Weast L (1989) CRC Handbook of chemisity and physics. CRC Press, Boca Raton

Westerhoff P, James J (2003) Nitrate removal in zero-valent iron packed columns. Water Res 37:1818–1830. https://doi.org/10.1016/s0043-1354(02)00539-0

Xing W, Li D, Li J, Hu Q, Deng S (2016) Nitrate removal and microbial analysis by combined micro-electrolysis and autotrophic denitrification. Bioresour Technol 211:240–247. https://doi.org/10.1016/j.biortech.2016.03.044

Xu H, Li Y, Ding M, Chen W, Wang K, Lu C (2018) Simultaneous removal of dissolved organic matter and nitrate from sewage treatment plant effluents using photocatalytic membranes. Water Res 143:250–259. https://doi.org/10.1016/j.watres.2018.06.044

Yang Z, Ma Y, Liu Y, Li Q, Zhou Z, Ren Z (2017) Degradation of organic pollutants in near-neutral pH solution by Fe-C micro-electrolysis system. Chem Eng J 315:403–414. https://doi.org/10.1016/j.cej.2017.01.042

Ying D, Peng J, Xu X, Li K, Wang Y, Jia J (2012) Treatment of mature landfill leachate by internal micro-electrolysis integrated with coagulation: a comparative study on a novel sequencing batch reactor based on zero valent iron. J Hazard Mater 229-230:426–433. https://doi.org/10.1016/j.jhazmat.2012.06.037

Zhang Y, Douglas GB, Pu L, Zhao Q, Tang Y, Xu W, Luo B, Hong W, Cui L, Ye Z (2017) Zero-valent iron-facilitated reduction of nitrate: chemical kinetics and reaction pathways. Sci Total Environ 598:1140–1150. https://doi.org/10.1016/j.scitotenv.2017.04.071

Zhang Y, Li J, Bai J, Li X, Shen Z, Xia L, Chen S, Xu Q, Zhou B (2018) Total organic carbon and total nitrogen removal and simultaneous electricity generation for nitrogen-containing wastewater based on the catalytic reactions of hydroxyl and chlorine radicals. Appl Catal B Environ 238:168–176. https://doi.org/10.1016/j.apcatb.2018.07.036

Zhou H, Lv P, Shen Y, Wang J, Fan J (2013) Identification of degradation products of ionic liquids in an ultrasound assisted zero-valent iron activated carbon micro-electrolysis system and their degradation mechanism. Water Res 47:3514–3522. https://doi.org/10.1016/j.watres.2013.03.057